Enhanced Electromechanical Resilience and Mechanism of the Composites-coated Fabric Sensors with Crack-induced Conductive Network for Wearable Applications

Xi Wang[1], Qiao Li[2],, Xiaoming Tao[3], **

[1]Engineering Research Center of Digitized Textile & Apparel Technology, Ministry of Education, College of Information Science and Technology, Donghua University, Shanghai 201620, China

[2]Key Laboratory of Textile Science & Technology, Ministry of Education, College of Textiles, Donghua University, Shanghai 201620, China;

[3]Institute of Textiles and Clothing, The Hong Kong Polytechnic University, Hong Kong;

**Correspondence: qiaoli@dhu.edu.cn; xiao-ming.tao@polyu.edu.hk*

Abstract

Conductive composites-coated fabric sensors are favorable sensing elements for wearable applications. However, rheology of composites ingredients has been causing inaccuracy due to high hysteresis and low instantaneity in real-time measurements. To address this problem, a composites-coated fabric-based strain sensor was fabricated and studied. A physical pretreatment scheme was designed to produce cracked surface morphology on the conductive composites film, yielding a stable conductive network. Results showed that this scheme can significantly lower the electrical hysteresis of the sensors by about 35% and effectively reduce electrical and mechanical relaxation, hence notably improved electromechanical resilience of the sensors. It’s also found that the linear strain-resistance property of the sensors was largely retained after pretreatment. Sensing mechanism of the cracked sensors was further derived to understand the results. Through all the observations and application prospect demonstrated by two sensing belts, it’s suggested that cracking can be considered to improve sensing performance for other coated fabric flexible sensors.

Keywords: conductive composites, coated fabric strain sensor, electromechanical resilience, sensing mechanism, wearable application

1. Introduction

Various textile materials with electronic functions have been designed and fabricated to achieve seamless integration and compliant interaction with the zoetic, soft, curved, and dynamically deformed human bodies[1-4]. Thanks to the merits of ease fabrication, large freedom of design and compliant interactions with the human body, the conductive fabric have been making towards the generation of electronic textiles, which are increasingly preferred in the field of wearables and enabling the advent of a large number of delicate wearable components or devices such as fabric electrodes[5], circuits[6, 7], antennas[8], sensors and actuators[9-11], as well as energy harvesting elements [12-15]. Compared to the "bulky, stiff and brittle" conventional sensors and those based on plastics or elastomers [16, 17], the conductive fabric materials are in soft, deformable and porous formats[18], hence frequently implemented in numerous human-centered applications, such as continuous, long-term health monitoring system[16, 17, 19], human-machine interface[20], as well as artificially electronic skin[5, 9, 16, 17].

There are two major ways to realize electronic fabrics, either to weave, knit, stitch or embroider conductive fibers (or threads) into fabric structures[6, 21-24], or to coat/deposit functional materials, especially polymers and carbon (or graphite) based conductive composites [25-28] on the three primary textiles, i.e., woven, knitted and nonwovens. Recently and with the printing technology, there has been rapid emergence of enormous conductive fabrics for specific usages, owing to its relative ease of large-scale fabrication and extreme freedom of design in arbitrary configurations of conductive tracks on the fabric substrate [29-32]. Published works have been frequently and extensively demonstrating the feasibility of diverse electronic functions as well as excellences of coated knitted fabrics, such as extreme extensibility (up to 500%), elasticity (up to 100%) and flexibility[10, 33, 34], which were endowed by the inner interlaced yarns in a series of connected three-dimensional (3D) loops. For instance, fabric strain sensors have been reported [35-38], along with experimental works showing that their sensing behaviors have reached a level similar to or even better than elastomeric sensors over recent years particularly from aspect of durability with large mechanical strain. However, the drawbacks of those sensors, especially the high hysteresis and drifting of electrical signals over time, have been causing instantaneous error of sensors and preventing them from accurate real-time application scenarios. Some researchers tended to eliminate the so-caused error via building mechanical or electromechanical models for those sensors[39-42], but there is still lack of successful validity verifications in working conditions. Recently, some works on flexible sensors have indicated that the non-beautiful cracks on the conductive material could also be utilized to reduce composites' rheological deformation during stretch, which may be incorporated to improve sensing performance [43-48].

To quantitatively determine the improvement of electro-mechanical resilience of the fabric-based flexible sensors, in this work, a coated fabric strain sensor is fabricated. Physical pretreatment is introduced to generate stable cracks on the composites film, and the electromechanical resilience of the sensors before and after pretreatment are compared. The new sensing mechanism of the pretreated sensor are then derived and further studied to understand the observations. Finally, the application prospect of the optimized sensors is demonstrated by two sensing belts, i.e., mounted on abdomen to monitor breath rate and on the belly of biceps brachii to detect localized strain of the upper limb during biceps curls in real-time. From all the results and tests, it's recommended that the proposed method of pretreatment can be utilized in improvement of instantaneity and optimization of sensing hysteresis for other flexible coated sensors for wearable applications.

2. Material and Methods

2.1. Conductive composite material

Materials for coated fabrics range in their electrical conductivities from insulating to highly conductive, i.e., 10^{-10} - 10^{5} S cm^{-1}, such as conducting polymers, carbon nanocomposites, as well as metal films. In this work, carbon black nanoparticles (Carbon ECP600JD, Akzo Nobel) with a weight content of 9% were fully mixed with dimethyl silicone elastomer (ELASTOSIL LR6200 A and B, Wacker Chemie AG, Germany) to form the conductive composite with a favorable volume resistivity in the order of kOhm [38].

2.2. Knitted fabric substrates

A single jersey knitted fabric (from Sunikorn Knitters Limited, Hong Kong) constructed by 83% polyamide with a linear density of 702D/60f and 17% spandex with a linear density of 40D/4f was selected as the fabric substrate, whose weight was 195 g m^{-2} with a density of 43 courses cm^{-1} and 22 wales cm^{-1}. The knitted fabric was firstly cleaned with 1g L^{-1} non-ionic detergent (Lentol B) at 60°C for 30 min and secondly rinsed thoroughly, followed by dehydration and drying at 60°C for 15 min.

2.3. Fabrication of the fabric strain sensors

Rationale of the fabric-based sensors is to improve compliance and breathability of elastomeric or plastic electronics, which are currently the majority of the flexible wearable devices. In this work, fabric strain sensors were fabricated and studied. The conductive composite was firstly uniformly coated twice on the knitted fabric substrates with a screen-printing machine (Guangdong Ever Bright Printing Machine Fty Ltd, Guangdong, China). The pre-tension was controlled at 1.2 N and the coating area was 5 mm*5 mm along the longitudinal (wale) direction. The coated fabric was then cured at 100 ℃ for one hour. After that, the conductive mixture became stiffer from a liquid state to a solid film as the silicone oil evaporated. Finally, two parallel soft electrodes (silver nanoparticles-coated polyamide yarn, purchased from Xiamen Unibest Import and Export Co., Ltd, China) were introduced and sewed into the conductive composites film, with a redetermined distance of 5 mm. In this work, 10 randomly selected resultant sensors are to be studied.

2.4. Experimental devices

To examine the electromechanical properties, fabric strain sensors were stretched by the Instron mechanical testing system (Model 5944, Instron, USA), while tension/load, electrical resistance and deformation were recorded simultaneously. For demonstration of conductive fabrics or smart wearable devices based on the sensors, Keithley 2010 multimeter was utilized. Surface geometry of the conductive fabric was observed on a 3D optical measurement system (Alicona IFM G4, Brook-Anco Corporate, America).

2.5. Cracks generation and characterization of the sensors

To evaluate the electro-mechanical properties of the piezoelectrical sensors, a testing protocol of calibration shall be adopted. In fact, most reported soft resistive-type strain sensors went through a number of prior loading-unloading cycles to stabilize their sensing performances. In this work and to reduce rheological effect the composites on the fabric strain sensors during deformation, physical pretreatment protocol was implemented to generate cracks on the conductive composites film. The obtained 5 mm fabric strain sensors went through 5 cycles of loading-unloading up to 100% strain (pre-determined according to experience) to make fibers sufficiently oriented in the direction of stretch as well as to generate and stabilize cracks on the conductive composites film. After that, the cracked fabric strain sensors were evaluated via calibration and relaxation test. To better illustrate the enhancement of electromechanical resilience, a 3-stage testing protocol was designed with the aforementioned Instron 5944. Aside from the 5-cycles of pretreatment, the electro-mechanical properties of the fabric strain sensors will be evaluated within the 10 cycles of calibration at 120 mm/min to 60% strain and 15-min holding stage at 60% strain (**Figure 1**). These 2 stages are for characterizing instantaneity of the sensors. The strain of 60% in calibration phase was designed according to the average extension range of human skin from 3% to 55% [54], while the 15-min holding stage is to sufficiently examine the tension and resistance relaxation at the strain of 60% [34, 42]. In this work, fabric strain sensors with or without pretreatment stage will be evaluated and compared.

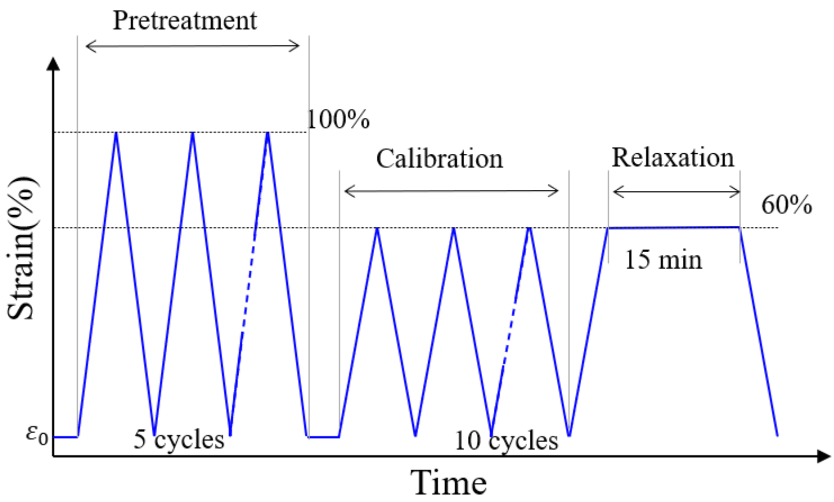

Figure 1 Protocol of test, consisting of 3 parts, i.e., pretreatment, calibration and relaxation

To characterize the mechanical resilience of the knitted fabric substrate as well as the electromechanical resilience of the printed sensors, sensitivity, stiffness, hysteresis and relaxation rate are to studied. Sensitivity is defined as increment of resistance rate subjected to unit strain. Stiffness is determined along the working direction, i.e., along the wale direction of the fabric strain sensors. Mechanical hysteresis of the knitted fabric Hy_F is defined as $\frac{|F_{\varepsilon_0 up}-F_{\varepsilon_0 down}|_{max}}{F_{max}-F_{min}} \times 100(\%)$, where $|F_{\varepsilon_0 up} - F_{\varepsilon_0 down}|_{max}$ is the largest difference in tension between the uploading and down-loading cycles, F_{max} and F_{min} are the maximum and minimum tension, respectively. Similarly, the electrical hysteresis Hy_R is defined as $Hy_R = \frac{|R_{\varepsilon_0 up}-R_{\varepsilon_0 down}|_{max}}{R_{max}-R_{min}} \times 100(\%)$, (where $|R_{\varepsilon_0 up} - R_{\varepsilon_0 down}|_{max}$ is the maximum difference in resistance between the uploading and down-loading conditions, R_{max} and R_{min} are the highest and lowest electrical resistances, respectively). Furthermore, the tension loss/resistance reduction over the 15-min relaxation stage is examined to quantify the mechanical/electrical resilience, i.e., used as an index of attenuation intensity.

3. Results and Discussion

3.1. The Composites-coated Fabric Strain Sensors

As aforementioned, conductive composite was uniformly coated on the knitted fabric substrates along the wale direction with a screen-printing machine. Two electrodes were additionally sewed into the conductive layer with a distance of 5 mm, making the coated fabric a piezoresistive strain sensor (**Figure 2a**). A three-plied polyamide yarn coated by silver nanoparticles (**Figure 2b**) was chosen as the conductive electrodes for its low resistance (~3.4 $\Omega.cm^{-1}$), good flexibility (Young's modulus of 0.531 GPa) and favorable durability (tensile stress 159.2 MPa at 30% strain, satisfying mechanical requirements of the sewing). As demonstrated in previous work of our group, also seen from Figure S1 in supporting information, this design of sensor shows negligible shift among cycles. For this work, we use the 100^{th} cycle for characterization of strain-load and strain-resistance properties. **Figure 2c-d** plot the representative electro-mechanical behavior of the fabric sensor within working range (5%~60%) during calibration.

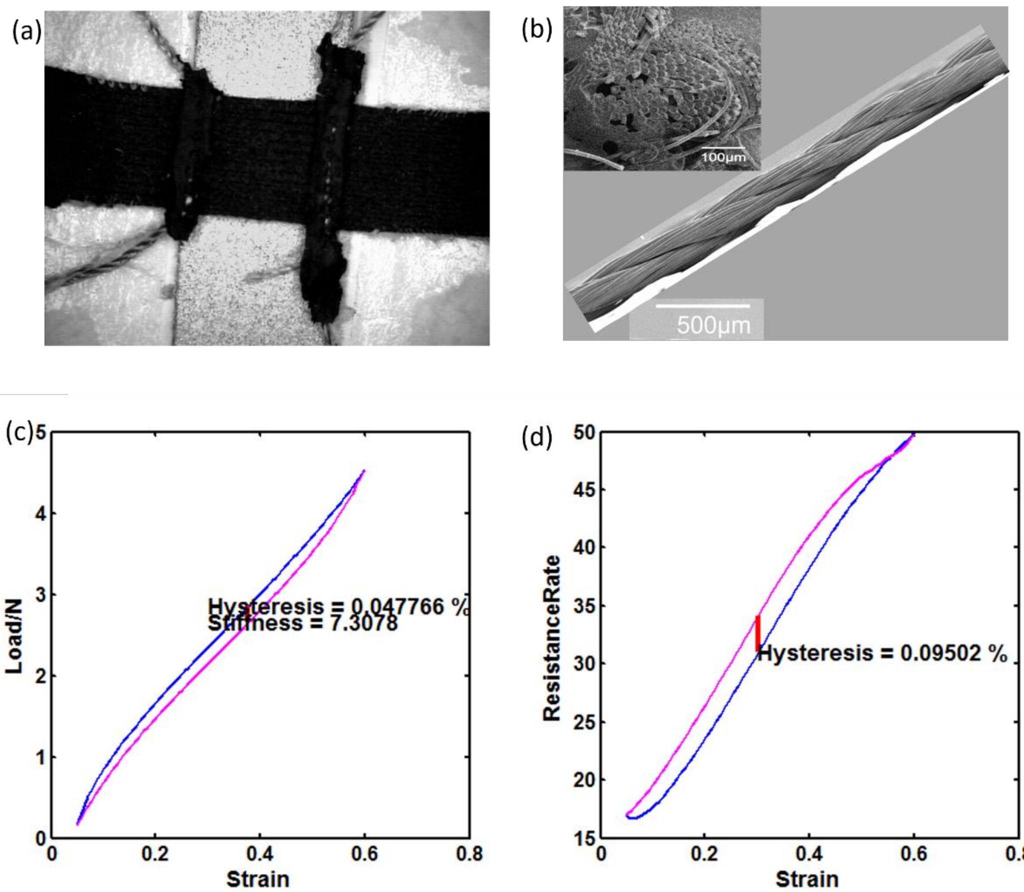

Figure 2. Fabric strain sensor. (a) Fabric strain sensor with two electrodes integrated into the conductive fabric; (b) SEM images of the electrode; Typical strain-load curve (c) and strain-resistance rate curve (d) acquired during calibration stage.

Moreover, previous works have shown that the fabric strain sensors response in ~0.01ms [33], and are capable of serving under a fatigue limit of about 100,000 cycles for a fairly broad working range of 60%. These merits make FSSs feasible and suitable for human daily-wear equipment such as shoes, shirts and belts. The strain gauge factor of the FSS can be adjusted according to application requirements [37]. The measuring error of FSS can be controlled within 5% and hysteresis was as low as ±3.5% [34].

Surface morphology of the sensor was further plotted in **Figure 3**, in which **Figure 3a-c** presents one typical sample with its front side, back side, and cross-sectional images in the transverse (course) and longitudinal (wale) cases, respectively. Thickness of the knitted substrate was 444(±5) μm while conductive composite was only about 23 μm. Moreover, the conductive fabric was observed constructed by a network with cell size of 219 μm and 229 μm, determined by that of the printing mesh, in the transverse (course) and longitudinal (wale) directions, respectively. The non-flat surface was confirmed in the cross-sectional images (**Figure 3c**) as well as quantitatively featured through investigation on its primary profile, surface waviness, and surface roughness on a 3D optical measurement system (**Figure 3d**). However, according to knitted fabric structure observed from front side (**Figure 3e**) and cross-sectional SEM (**Figure 3f**), the micro-order concave-convex network were with a mean unit size of 245 μm and 270 μm in the course and wale directions, respectively. The thin thickness of the composites film compared to the fabric substrates as well as the discrepancies in cell size of the composites film and knitted fabric substrates would inevitably make the composites surface easily teared into cracked networks at larger strains, due to the stress concentration, either at locations of weak/thin composites film or near the bonding locations of the 2 materials.

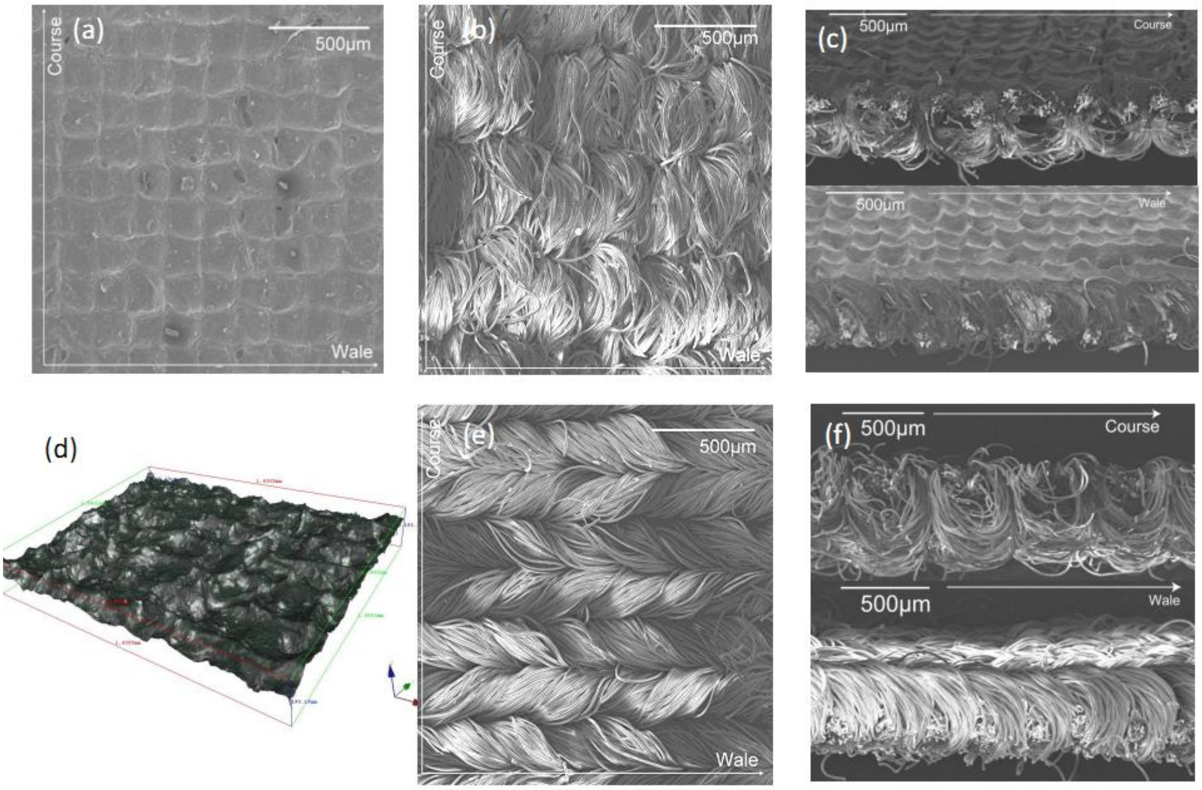

Figure 3. Carbon nanocomposite-coated fabric strain sensor: (a) front side/coated composites, (b) back side/knitted fabric, (c) cross-sectional images in the course and wale directions, (d) 3D optical image; (e) and (f) are the front side and cross-sectional images in the course and wale cases of original knitted fabric substrate (before coating).

3.2. Morphology of the cracked fabric strain sensors

As elaborated above, the fabric strain sensors, consisting of a knitted fabric as the supporting layer and the continuous carbon nanocomposites as the conductive layer, is expected to transfer the continuous surface of the sensor to a cracked sensing network, by which means the sensing mechanism maybe altered. SEM images of the sensor under different strain (0% to 30% and 60%) are demonstrated in **Figure 4 a-c** to characterize the cracked composites surface. Two distinctive phenomena can be observed from the figure. First, radial micro-cracks were successfully formed on the conductive layer after pretreatment. The number and size of the micro-cracks becomes more and obvious at larger strain. Secondly, it can be further calculated that the local strain distribution in both wale and course cases were uneven with unidirectional applied strain [49], reflecting an effect of plane Poisson's ratio. With micro-cracks on the composite layer, it's no longer appropriate to directly implement Simmons' equation on tunneling electrical resistance [50] to study the sensing mechanism.

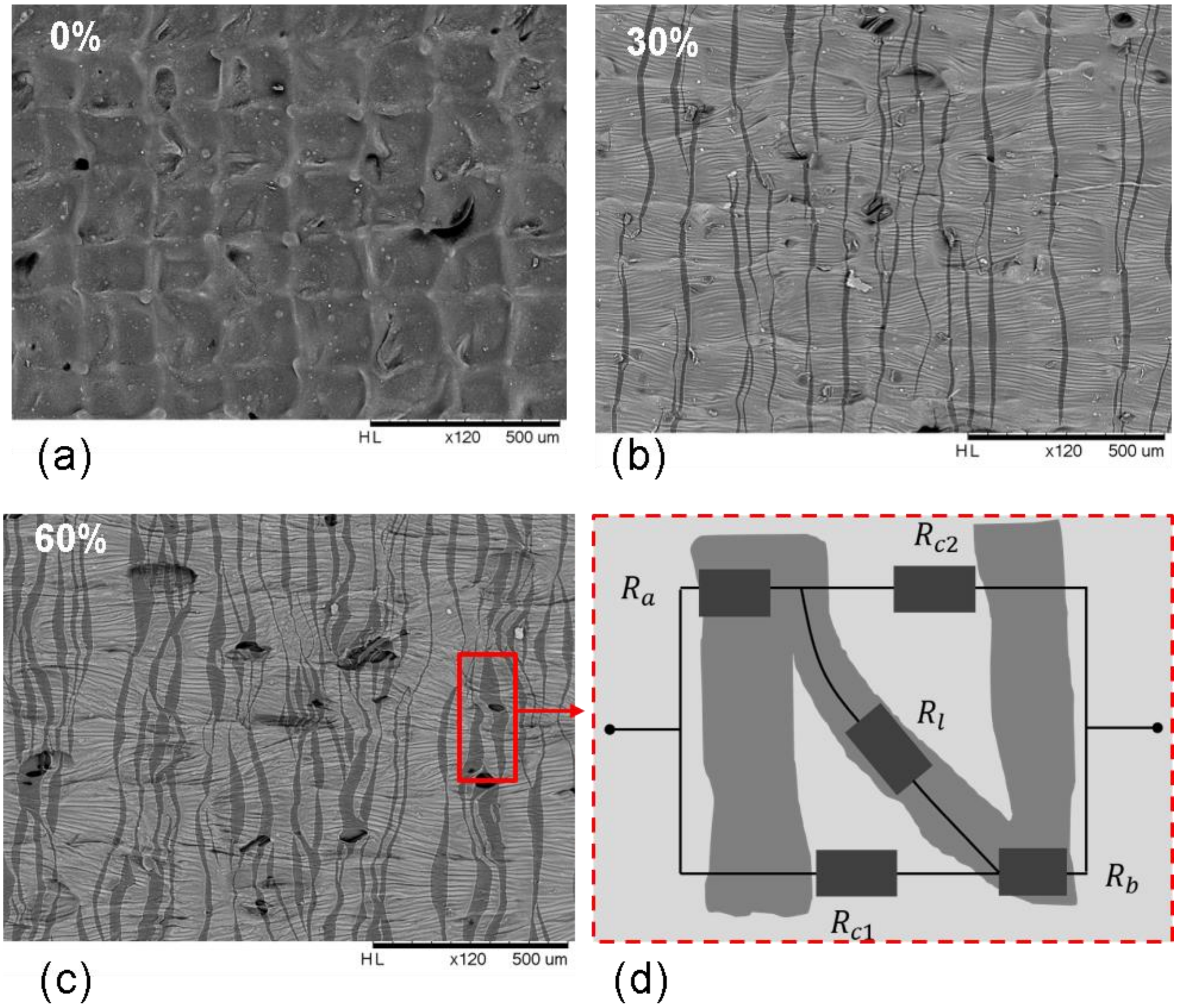

Figure 4. Cracks on the composites film of the fabric strain sensors: (a)-(c) SEM images under different strain from 0% to 60%; (d) resistance model of the crack structure

3.3. Enhanced electromechanical resilience of the cracked fabric strain sensors

To determine the improvement of electromechanical resilience, 10 randomly selected sensors were studied during calibration and relaxation. Comparisons were made between electromechanical properties for the sensors before and after pretreatment (i.e., with or without cracks formed on composites film), as can be demonstrated by sample No.3 in **Figure 5** and summarized in **Table 1**.

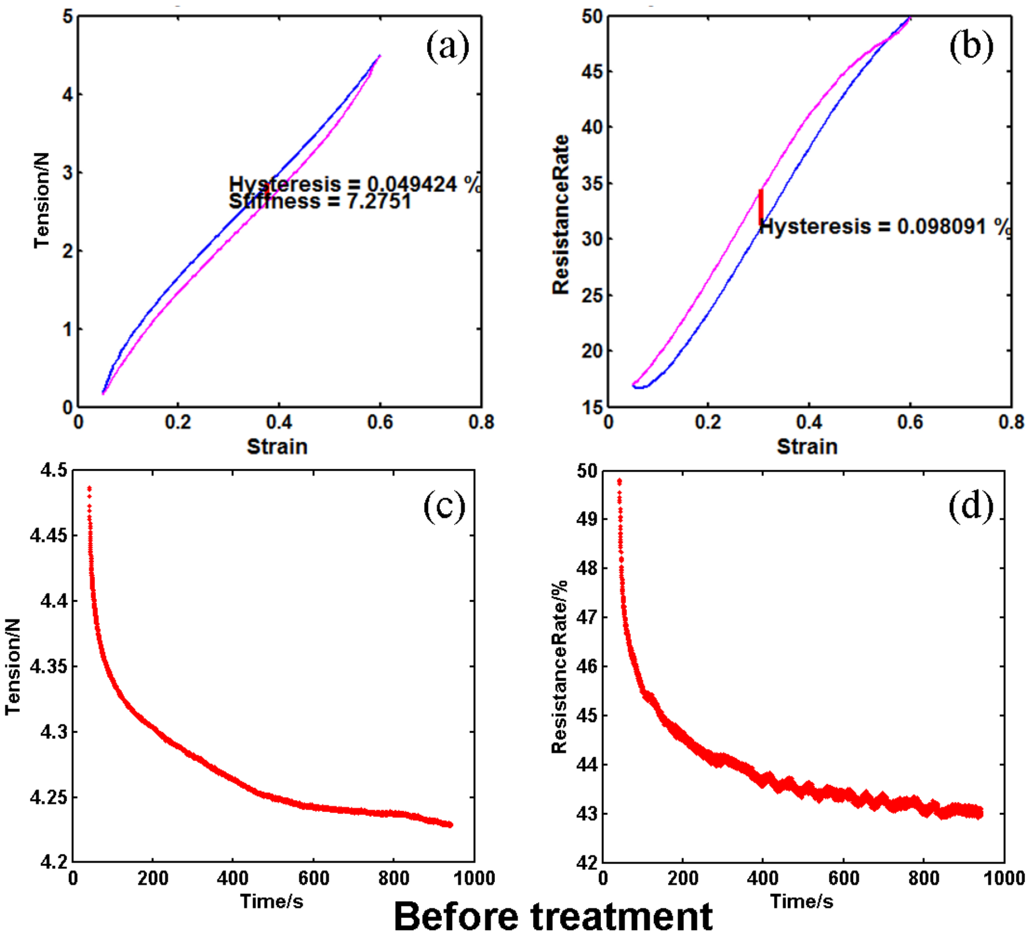

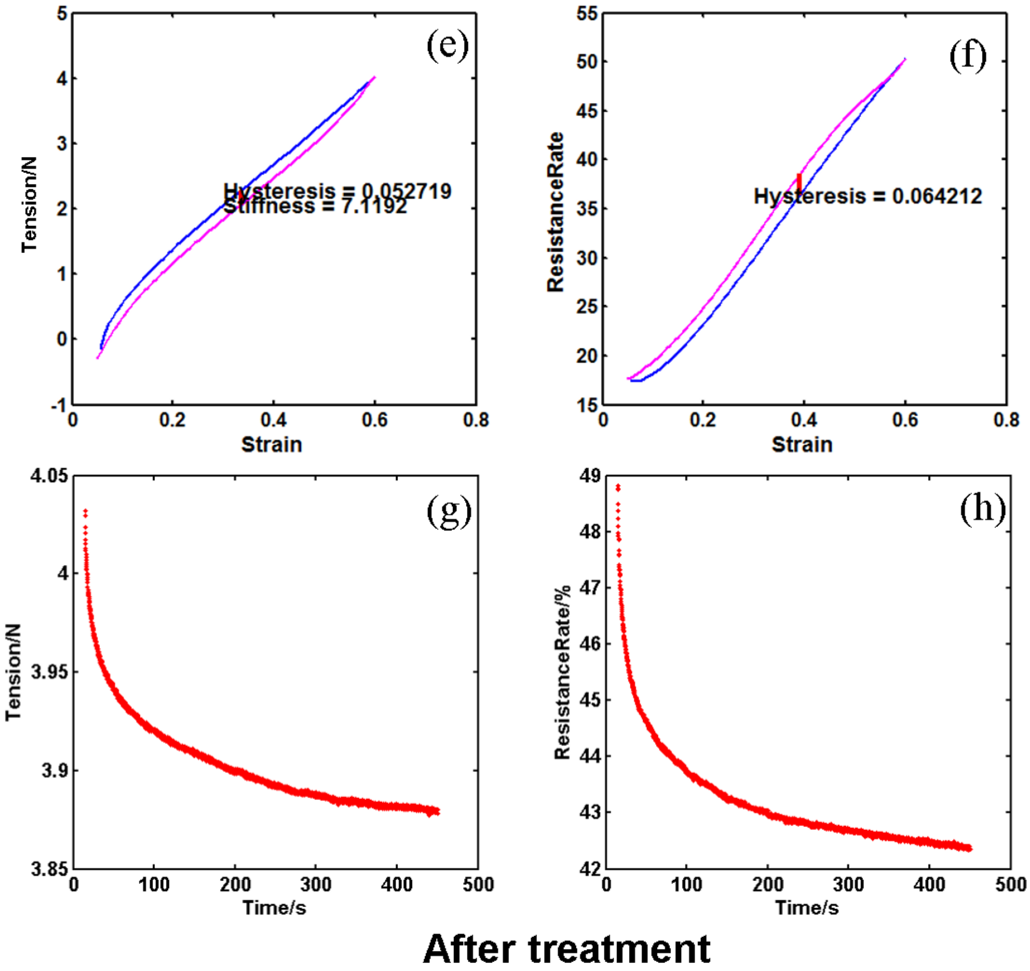

Figure 5 Typical characterization of strain-tension (a), strain-resistance (b), tension relaxation (c), and resistance relaxation (d) property of the fabric resistive sensor No.3 before pretreatment and that after pretreatment (e)~(h).

Table 1 Comparison between sensors' electromechanical properties before and after pretreatment at 100% strain.

\	Sensitivity	Stiffness /N	Mechanical hysteresis /%	Electrical Hysteresis /%	Mechanical relaxation /%	Electrical relaxation /%
Before pretreatment	59.64(±0.30)	7.28(±0.03)	4.82(±0.08)	9.36 (±0.28)	6.12 (±0.49)	7.10(±0.41)
After pretreatment	58.51(±0.35)	7.13(±0.02)	5.16(±0.08)	6.03 (±0.19)	4.53 (±0.32)	6.49 (±0.50)

Several conclusions can be made. First, after pretreatment and with cracks formed on the conductive composite film, stiffness of the sensor decreased from 7.28 to 7.13, since the broken conductive composites no longer provide force of resilience and the knitted fabric substrate undertook more tension. For the same reason, it can also be observed that mechanical hysteresis slightly increased. Secondly, the strain-resistance hysteresis significantly reduced by about 35% from 9.36%, which means pretreatment can effectively reduce the strain-resistance hysteresis and improve the repeatability of sensors (Figure S1, supporting information). This is in accordance with the result that when cracks formed after pretreatment, sensing mechanism of the sensor with respect to mechanical strain was altered to the switch on-and-off effect of the conductive network as elaborated above. Analysis of variation (ANOVA) was further performed on the observed stiffness, mechanical hysteresis and electrical hysteresis of untreated and pretreated sensors, to show the effectiveness of the crack generation. It's observed that the p-values were as low as $2.2*10^{-4}$, $2.4*10^{-5}$, $8.1*10^{-13}$, respectively, showing that the decrease in stiffness, increase in mechanical hysteresis and decrease in electrical hysteresis were significant. Thirdly, when the rheological material, i.e., composite film has little change to deform in the switch network, the relaxed tension over the 15-min hold stage at strain 60% was found improved by about 26%, from 6.12% to 4.53%. 8.6% improvement can be found with the electrical resistance relaxation, which reduced from 7.10% to 6.49%. These results suggest that, for the coated flexible sensors with knitted fabric substrate, it's effective to lower sensing delay through producing stable cracks on the coated conductive composite film.

However, it's interesting that the cracked fabric strain sensors revealed similar strain-resistance relationship as illustrated in **Figure 5**. The underlying mechanism of this observation shall be confirmed.

3.4. Strain-resistance sensing mechanism of the cracked fabric strain sensor

According to the structure of the fabric strain sensors, deformation of continuous conductive composites is caused by the extension of the knitted fabric substrate. To describe the resultant deformation of the whole sensor, plane deformation response under 2D extension was considered. Let e_1 and e_2 be the strain exerted on the conductive composite film by the knitted fabric, the resultant strain ε_1, ε_2 and ε_3 in the length and width directions, then the resultant strain of the wale, course, as well as thickness directions can be derived as:

$$\begin{bmatrix} \varepsilon_1 \\ \varepsilon_2 \\ \varepsilon_3 \end{bmatrix} = \begin{bmatrix} 1 & -\nu & -\nu \\ -\nu & 1 & -\nu \\ -\nu & -\nu & 1 \end{bmatrix} \cdot \begin{bmatrix} e_1 \\ e_2 \\ 0 \end{bmatrix} \quad (1)$$

where e_1 and e_2 are the strains exerted by knitted fabric substrate in wale and course directions, respectively; ν is Poisson's ratio of this conductive composite. Easy to understand that e_3 is naturally zero since there is no mechanical restraint in the thickness direction. Since it's observed that the thickness of the conductive fabric was 467(±4) µm, of which the knitted substrate was 444(±5) µm and the conductive composite was about 23 µm, it's reasonable to assume that the plane Poisson's ratio effect of the knitted fabric substrate dominates the strain shrink of the packaged sensor in width direction. Hence, we get

$$\varepsilon_2 = -\mu\varepsilon_1, \varepsilon_3 = -\nu\varepsilon_1\left(\frac{1-\mu}{1-\nu}\right) \quad (2)$$

where μ is the plane Poisson's ratio of the packaged sensor. From macroscopic view and according to Ohm's Law, the resistance of the sensor with respect to the strain in the length direction (ε_1) can be written as

$$R = \rho\frac{L}{S} = \rho\frac{L_0(1+\varepsilon_1)}{S_0(1-u\varepsilon_1)\left(1-\nu\varepsilon_1\left(\frac{1-u}{1-\nu}\right)\right)} \quad (3)$$

Although the existence of Poisson's ratio makes the function $R(\varepsilon_1)$ theoretically nonlinear, with Poisson's ratio $\nu = 0.5$ and plane Poisson's ratio $u \approx 0.1$ as observed, it's easy to find that the strain-resistance curve of $R(\varepsilon_1)$ approaches linear style within working range of 5%~60%. This is the basic sensing mechanism of the non-cracked fabric strain sensors, as have been depicted in **Figure 2 d**.

It's not this case, however, when cracks formed on composites film. For cracked fabric strain sensors, initial cracks were enlarged with strain during stretch. The contact of adjacent conductive particles (i.e., carbon black nanoparticles) was decreased when the gaps become wider, resulting in narrower conductive pathways. When the stretch force is released, the crack gaps turn back to be narrow, the conductive pathways recover as the islands are gradually connected. According to the resistance model of the crack structure as in **Figure 4d**, the electrical resistance of the unit can be given as

$$R = \frac{R_A R_C + R_B R_l}{R_C + R_l} \tag{4}$$

where $R_A = \frac{R_a R_{c1}}{R_a + R_{c1}} + \frac{R_b R_{c2}}{R_b + R_{c2}}$, $R_B = \frac{(R_a + R_{c2})(R_b + R_{c1})}{R_a + R_b + R_{c1} + R_{c2}}$, $R_C = \frac{(R_a + R_{c1})(R_b + R_{c2})}{R_a + R_b + R_{c1} + R_{c2}}$. R_a, R_b and R_l were reginal resistance, while R_{c1} and R_{c2} were resistance of broken conduction by gaps. In this case, R_a, R_b and R_l were naturally in linear relationship with applied strain, according to the sensing mechanism with continuous composites film. The gaps resistance R_{c1} and R_{c2} on the other hand were of higher magnitude than R_a, R_b and R_l, leading to the approximation of the electrical resistance of the unit

$$R = R_a + R_b + R_l \tag{5}$$

It's easy to understand that for the cracked fabric strain sensors, linkage resistance R_l now took parallelogram deformation, which made its resistance variated much smaller than that during uniaxial stretch. This explains the slightly smaller sensitivity for the cracked fabric strain sensors, as shown in **Table 1**. Moreover, given more stable R_l and that R_a, R_b are approximately linear functions of applied strain, the overall strain-resistance behavior would definitely exhibit in similar manner compared to that of the uncracked sensors, as shown in **Figure 5**.

This finding shows that, the fabric strain sensors' electromechanical resilience can be notably improved through generation of cracks on composites film, while the sensing properties were generally maintained.

It's worth mentioning that, this method is based on crack-generation, which would definitely raise 2 major issues: first, the cracked surface fails the waterproofness of coated fabric sensor, making it inappropriate for next-to skin applications; second, for coated strain sensors, the rougher surface would make them of less resistance to wear, which is common for embedded elements in apparels. Both would narrow the application horizon of those sensors.

4. Application

The flexible fabric resistive strain sensors, as with large working range (0%~60%) with good repeatability (>100,000 cycles) and optimized low hysteresis (~6%) after pretreatment [34, 37, 38], are now suitable to be utilized to detect mechanical deformation in practical applications with the capability of conforming to the soft and curved human skins. As a proof-of-concept, two types of sensing belts were designed for wearable application, where the length of sensing belts were properly controlled to ensure a safety pressure of not higher than 4.3 kPa on human body, the effect of the out-plane pressure on the sensor could introduce a measuring error of not higher than 0.1% in resistance ratio, and was thus negligible. Ethic committee of the Hong Kong Polytechnic University reviewed and approved the research, which was conducted in accordance with the principles embodied in the Declaration of Helsinki and in accordance with local statutory requirements. 2 subjects were enrolled (one for each type of belt) and informed of the information collected for study. Signed consents were obtained prior to tests.

For the first application, one single sensor was incorporated into an elastic belt for temporal monitoring of breath rate. As shown in **Figure 6a**, the belt can be mounted around the abdomen of a young and healthy subject, who kept standing in salience with normal respiration, while the variation of resistance over time during normal respiration was observed. It can be seen that the resistance rises as the subject inhale and drops for exhale. Breathing period and frequency can be easily observed through identifying the peaks and valleys of the curve. The average period is approximately 3 s for one normal breath, which is consistent with the time recorded by examiner by side. Furthermore, when the sensors are sensitive enough, heart rate can also be extracted using the Least Mean Square algorithm. The second application was a multi-sensor belt for continuously measurement of the circumferential variation of upper limbs in motion. Six fabric stretchy sensors with a sensing area of 8 mm*25 mm were assembled and carried by a soft belt with optimized elastic resilience. Enameled copper wire in a zigzag pattern was used to electrically and physically connect the n sensors to outer circuits in a '$n+1$' array, that is, one electrical wire was adopted as ground line and the others of n th end of sensors output the n th signal (**Figure 6b**). When mounted on the location of the belly of the biceps brachii on the subject's upper arm (**Figure 6c**), the sensing belt can be used to track the circumferential strains during movements of flexions and extensions during biceps curls of the subject. As can be observed in **Figure 6d**, the sensing belt revealed an accuracy of less than 5% and an excellent linearity of 998‰ in calibration using INSTRON. The in-location circumferential strains can be further integrated around the belt to give the overall circumference, which reflects the variation in thickness of the voluntary muscle (biceps brachii) [34]. Overall, these applications suggest stable performance of the fabric strain sensors after pretreatment, which opens wider horizons in wearable field and bio-mechanical monitoring in sports.

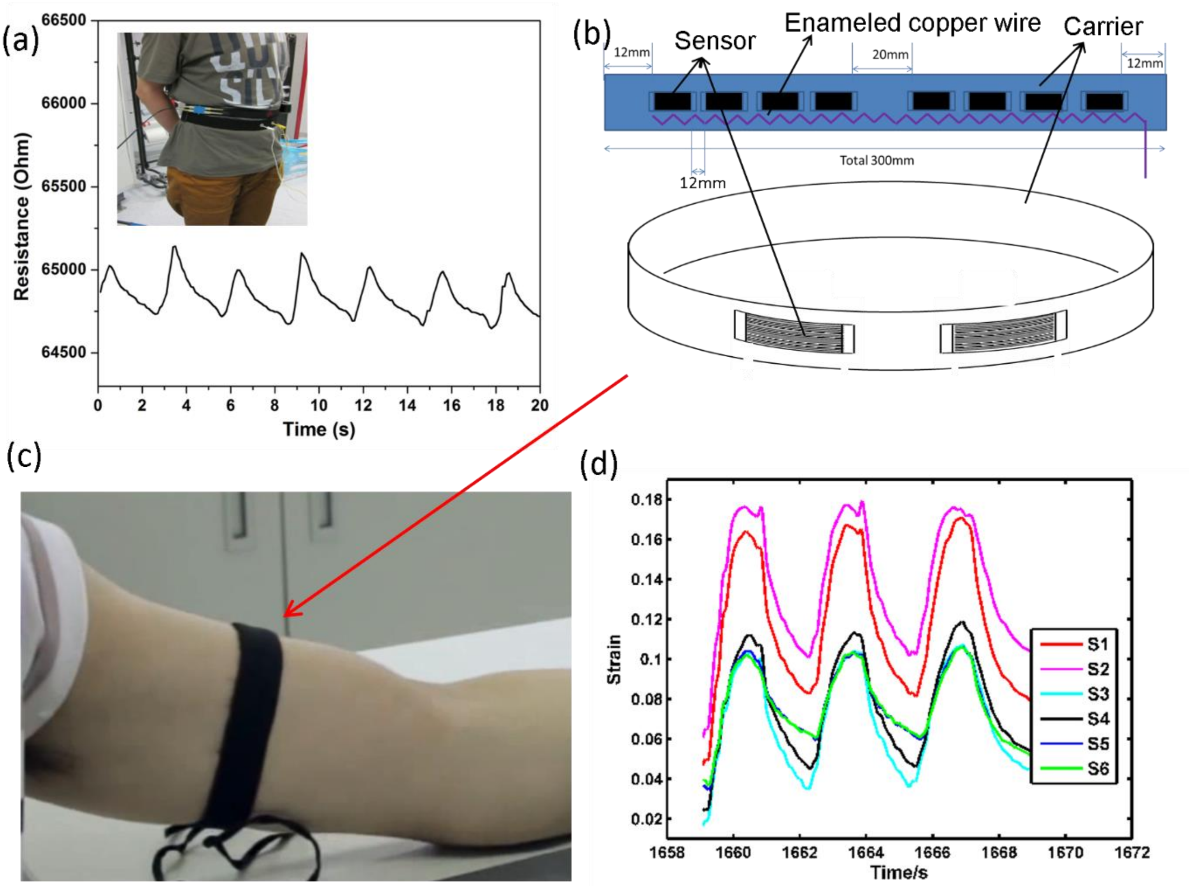

Figure 6. Applications of the pretreated fabric strain sensors. (a) sensing belt for respiration monitoring. (b)-(c) multiple sensors incorporated into the belt for measurement real-time circumferential strain during elbow flexion. (d) comparison between real and measured strain over time.

The above demonstrative studies involving human participants were performed with the informed consent of all the participants.

5. Conclusion

Coated conductive fabrics have been frequently studied all over the field of electronic textiles. However, due to rheology of materials, the sensing delay and repeatability have been preventing those novel sensors from accurate sensing applications.

Hence in this paper, a coated flexible strain sensor based on conductive composite and knitted fabric substrate were studied. Through physical pretreatment scheme at 100% strain, stable crack networks formed on the composites film of the sensors. It's then found that this pretreatment can significantly reduce the electrical hysteresis of the sensors by about 35%, also induced 26% smaller mechanical relaxation and 8.6% smaller electrical relaxation, hence effectively improved the instantaneity and electromechanical resilience of the sensors, making them more accurate. Moreover, according to the island-gap sensing mechanism model of the cracked sensors, the linear strain-resistance property was largely retained. The application prospect of the optimized sensors is preliminary demonstrated by two sensing belts, i.e., mounted on addomen to monitor breath rate and on the belly of biceps brachii to detect localized strain of the upper limb during biceps curls in real-time. It's recommended that the proposed method of pretreatment can be utilized in improvement of instantaneity and optimization of sensing hysteresis for other flexible coated sensors for wearable applications.

Acknowledgement

This research was funded by the National Natural Science Foundation of China (Grant No. 12002085, 51603039), sponsored by Shanghai Pujiang Program, and supported by the Fundamental Research Funds for the Central Universities, the Key Laboratory of Textile Science and Technology (Donghua University), Ministry of Education, as well as the Initial Research Funds for Young Teachers of Donghua University.

Conflict of Interest

The authors declare no conflict of interest.

References:

[1]. W. Zeng, L. Shu, Q. Li, S. Chen, F. Wang, and X. M. Tao, *Fiber-based wearable electronics: a review of materials, fabrication, devices, and applications.* Adv Mater, 2014. **26**(31): p. 5310-36.

[2]. Q. Li and X. M. Tao, *Three-dimensionally deformable, highly stretchable, permeable, durable and washable fabric circuit boards.* Proc Math Phys Eng Sci, 2014. **470**(2171): p. 20140472.

[3]. S. Kim, B. Lee, J. T. Reeder, S. H. Seo, S. U. Lee, A. Hourlier-Fargette, J. Shin, Y. Sekine, H. Jeong, Y. S. Oh, A. J. Aranyosi, S. P. Lee, J. B. Model, G. Lee, M. H. Seo, S. S. Kwak, S. Jo, G. Park, S. Han, I. Park, H. I. Jung, R. Ghaffari, J. Koo, P. V. Braun, and J. A. Rogers, *Soft, skin-interfaced microfluidic systems with integrated immunoassays, fluorometric sensors, and impedance measurement capabilities.* Proc Natl Acad Sci U S A, 2020. **117**(45): p. 27906-27915.

[4]. J. Xiong, J. Chen, and P. S. Lee, *Functional Fibers and Fabrics for Soft Robotics, Wearables, and Human-Robot Interface.* Adv Mater, 2020. **n/a**(n/a): p. e2002640.

[5]. C. L. Choong, M. B. Shim, B. S. Lee, S. Jeon, D. S. Ko, T. H. Kang, J. Bae, S. H. Lee, K. E. Byun, J. Im, Y. J. Jeong, C. E. Park, J. J. Park, and U. I. Chung, *Highly stretchable resistive pressure sensors using a conductive elastomeric composite on a micropyramid array.* Adv Mater, 2014. **26**(21): p. 3451-8.

[6]. K. Cherenack, C. Zysset, T. Kinkeldei, N. Munzenrieder, and G. Troster, *Woven electronic fibers with sensing and display functions for smart textiles.* Adv Mater, 2010. **22**(45): p. 5178-82.

[7]. Q. Li and X. M. Tao, *A stretchable knitted interconnect for three-dimensional curvilinear surfaces.* Textile Research Journal, 2011. **81**(11): p. 1171-1182.

[8]. M. L. Scarpello, I. Kazani, C. Hertleer, H. Rogier, and D. Vande Ginste, *Stability and Efficiency of Screen-Printed Wearable and Washable Antennas.* Ieee Antennas and Wireless Propagation Letters, 2012. **11**: p. 838-841.

[9]. X. Wang, Y. Gu, Z. Xiong, Z. Cui, and T. Zhang, *Silk-molded flexible, ultrasensitive, and highly stable electronic skin for monitoring human physiological signals.* Adv Mater, 2014. **26**(9): p. 1336-42.

[10]. L. Shu, T. Hua, Y. Wang, Q. Qiao Li, D. D. Feng, and X. Tao, *In-shoe plantar pressure measurement and analysis system based on fabric pressure sensing array.* IEEE Trans Inf Technol Biomed, 2010. **14**(3): p. 767-75.

[11]. X. T. Li, T. Hua, and B. G. Xu, *Electromechanical properties of a yarn strain sensor with graphene-sheath/polyurethane-core.* Carbon, 2017. **118**: p. 686-698.

[12]. W. Zeng, X. M. Tao, S. Chen, S. M. Shang, H. L. W. Chan, and S. H. Choy, *Highly durable all-fiber nanogenerator for mechanical energy harvesting.* Energy & Environmental Science, 2013. **6**(9): p. 2631-2638.

[13]. Weiyi Zhang, Qiang Liu, Shengyu Chao, Ruping Liu, Xi Cui, Yu Sun, Han Ouyang, and Zhou Li, *Ultrathin Stretchable Triboelectric Nanogenerators Improved by Postcharging Electrode Material.* ACS Applied Materials & Interfaces, 2021. **13**(36): p. 42966-42976.

[14]. Han Ouyang, Jingjing Tian, Guanglong Sun, Yang Zou, Zhuo Liu, Hu Li, Luming Zhao, Bojing Shi, Yubo Fan, Yifan Fan, Zhong Lin Wang, and Zhou Li, *Self-Powered Pulse Sensor for Antidiastole of Cardiovascular Disease.* Advanced Materials, 2017. **29**(40): p. 1703456.

[15]. Han Ouyang, Dongjie Jiang, Yubo Fan, Zhong Lin Wang, and Zhou Li, *Self-powered technology for next-generation biosensor.* Science Bulletin, 2021. **66**(17): p. 1709-1712.

[16]. D. Son, J. Lee, S. Qiao, R. Ghaffari, J. Kim, J. E. Lee, C. Song, S. J. Kim, D. J. Lee, S. W. Jun, S. Yang, M. Park, J. Shin, K. Do, M. Lee, K. Kang, C. S. Hwang, N. Lu, T. Hyeon, and D. H. Kim, *Multifunctional wearable devices for diagnosis and therapy of movement disorders.* Nat Nanotechnol, 2014. **9**(5): p. 397-404.

[17]. G. Schwartz, B. C. Tee, J. Mei, A. L. Appleton, D. H. Kim, H. Wang, and Z. Bao, *Flexible polymer transistors with high pressure sensitivity for application in electronic skin and health monitoring.* Nat Commun, 2013. **4**: p. 1859.

[18]. Qiao Li, Li‐Na Zhang, Xiao‐Ming Tao, and Xin Ding, *Temperature Sensors: Review of Flexible Temperature Sensing Networks for Wearable Physiological*

Monitoring (Adv. Healthcare Mater. 12/2017). Advanced Healthcare Materials, 2017. **6**(12): p. 1601371.

[19]. S. Lin, W. Yu, B. Wang, Y. Zhao, K. En, J. Zhu, X. Cheng, C. Zhou, H. Lin, Z. Wang, H. Hojaiji, C. Yeung, C. Milla, R. W. Davis, and S. Emaminejad, *Noninvasive wearable electroactive pharmaceutical monitoring for personalized therapeutics.* Proc Natl Acad Sci U S A, 2020. **117**(32): p. 19017-19025.

[20]. S. C. Mannsfeld, B. C. Tee, R. M. Stoltenberg, C. V. Chen, S. Barman, B. V. Muir, A. N. Sokolov, C. Reese, and Z. Bao, *Highly sensitive flexible pressure sensors with microstructured rubber dielectric layers.* Nat Mater, 2010. **9**(10): p. 859-64.

[21]. X. Lee, T. T. Yang, X. Li, R. J. Zhang, M. Zhu, H. Z. Zhang, D. Xie, J. Q. Wei, M. L. Zhong, K. L. Wang, D. H. Wu, Z. H. Li, and H. W. Zhu, *Flexible graphene woven fabrics for touch sensing.* Applied Physics Letters, 2013. **102**(16).

[22]. O. Atalay, W. R. Kennon, and M. D. Husain, *Textile-based weft knitted strain sensors: effect of fabric parameters on sensor properties.* Sensors (Basel), 2013. **13**(8): p. 11114-27.

[23]. T. Linz, M. von Krshiwoblozki, H. Walter, and P. Foerster, *Contacting electronics to fabric circuits with nonconductive adhesive bonding.* Journal of the Textile Institute, 2012. **103**(10): p. 1139-1150.

[24]. K. Cherenack and L. van Pieterson, *Smart textiles: Challenges and opportunities.* Journal of Applied Physics, 2012. **112**(9).

[25]. L. B. Hu and Y. Cui, *Energy and environmental nanotechnology in conductive paper and textiles.* Energy & Environmental Science, 2012. **5**(4): p. 6423-6435.

[26]. Sabyasachi Ghosh, Sayan Ganguly, Sanjay Remanan, and Narayan Ch Das, *Fabrication and investigation of 3D tuned PEG/PEDOT: PSS treated conductive and durable cotton fabric for superior electrical conductivity and flexible electromagnetic interference shielding.* Composites Science and Technology, 2019. **181**: p. 107682.

[27]. Jiefeng Gao, Junchen Luo, Ling Wang, Xuewu Huang, Hao Wang, Xin Song, Mingjun Hu, Long-Cheng Tang, and Huaiguo Xue, *Flexible, superhydrophobic and highly conductive composite based on non-woven polypropylene fabric for electromagnetic interference shielding.* Chemical Engineering Journal, 2019. **364**: p. 493-502.

[28]. N. Karim, S. Afroj, S. R. Tan, K. S. Novoselov, and S. G. Yeates, *All Inkjet-Printed Graphene-Silver Composite Ink on Textiles for Highly Conductive Wearable Electronics Applications.* Scientific Reports, 2019. **9**.

[29]. Z. H. Ma, W. Wang, and D. Yu, *Highly Sensitive and Flexible Pressure Sensor Prepared by Simple Printing Used for Micro Motion Detection.* Advanced Materials Interfaces, 2020. **7**(2).

[30]. B. A. Kuzubasoglu, E. Sayar, C. Cochrane, V. Koncar, and S. K. Bahadir, *Wearable temperature sensor for human body temperature detection.* Journal of Materials Science-Materials in Electronics, 2021. **32**(4): p. 4784-4797.

[31]. Yang Wei, Russel Torah, Yi Li, and John Tudor, *Dispenser printed capacitive proximity sensor on fabric for applications in the creative industries.* sensors and actuators a physical, 2016. **247**: p. 239-246.

[32]. S. Masihi, M. Z. Atashbar, M. Panahi, D. Maddipatla, A. K. Bose, X. Zhang, A. J. Hanson, V. Palaniappan, B. B. Narakathu, and B. J. Bazuin, *A Novel Printed Fabric Based Porous Capacitive Pressure Sensor For Flexible Electronic Applications*, in *IEEE Sensors*. 2019.

[33]. F. Wang, B. Zhu, L. Shu, and X. M. Tao, *Flexible pressure sensors for smart protective clothing against impact loading.* Smart Materials and Structures, 2014. **23**(1).

[34]. X. Wang, X. M. Tao, R. C. H. So, L. Shu, B. Yang, and Y. Li, *Monitoring elbow isometric contraction by novel wearable fabric sensing device.* Smart Materials and Structures, 2016. **25**(12).

[35]. Xian Song, Xiaoting Liu, Yuxin Peng, Zhen Xu, Wenming Liu, Kai Pang, Jianxiang Wang, Liang Zhong, Qiang Yang, and Jun Meng, *A graphene-coated silk-spandex fabric strain sensor for human movement monitoring and recognition.* nanotechnology, 2021. **32**(21).

[36]. Waleri Root, Tom Wright, Barnaby Caven, Thomas Bechtold, and Tung Pham, *Flexible Textile Strain Sensor Based on Copper-Coated Lyocell Type Cellulose Fabric.* polymers, 2019. **11**(5).

[37]. Y. Y. Wang, T. Hua, B. Zhu, Q. Li, W. J. Yi, and X. M. Tao, *Novel fabric pressure sensors: design, fabrication, and characterization.* Smart Materials & Structures, 2011. **20**(6).

[38]. W. J. Yi, Y. Y. Wang, G. F. Wang, and X. M. Tao, *Investigation of carbon black/silicone elastomer/dimethylsilicone oil composites for flexible strain sensors.* Polymer Testing, 2012. **31**(5): p. 677-684.

[39]. L. H. Wang, C. G. Xu, and Y. L. Li, *Piezoresistive response to changes in contributive tunneling film network of carbon nanotube/silicone rubber composite under multi-load/unload.* Sensors and Actuators a-Physical, 2013. **189**: p. 45-54.

[40]. L. H. Wang and Y. Y. Han, *Compressive relaxation of the stress and resistance for carbon nanotube filled silicone rubber composite.* Composites Part a-Applied Science and Manufacturing, 2013. **47**: p. 63-71.

[41]. X. Wang, B. Yang, Q. Li, F. Wang, and X. M. Tao, *Modeling the stress and resistance relaxation of conductive composites-coated fabric strain sensors.* Composites Science and Technology, 2021. **204**.

[42]. Y. H. Gao, Q. Li, A. H. Dong, F. Wang, and X. Wang, *Characterizing the Resistance Relaxation of the Fabric-based Resistive Sensors Based on an Electro-mechanical Model.* Sensors and Actuators a-Physical, 2020. **310**.

[43]. L. Rodriguez-Tembleque, F. Garcia-Sanchez, E. Garcia-Macias, F. C. Buroni, and A. Saez, *Crack-induced electrical resistivity changes in cracked CNT-reinforced composites.* Theoretical and Applied Fracture Mechanics, 2020. **106**.

[44]. B. Park, J. U. Kim, J. Kim, D. Tahk, C. Jeong, J. Ok, J. H. Shin, D. Kang, and T. I. Kim, *Strain-Visualization with Ultrasensitive Nanoscale Crack-Based Sensor Assembled with Hierarchical Thermochromic Membrane.* Advanced Functional Materials, 2019. **29**(40).

[45]. C. J. Lee, K. H. Park, C. J. Han, M. S. Oh, B. You, Y. S. Kim, and J. W. Kim, *Crack-induced Ag nanowire networks for transparent, stretchable, and highly sensitive strain sensors.* Scientific Reports, 2017. **7**.

[46]. D. Kang, P. V. Pikhitsa, Y. W. Choi, C. Lee, S. S. Shin, L. F. Piao, B. Park, K. Y. Suh, T. I. Kim, and M. Choi, *Ultrasensitive mechanical crack-based sensor inspired by the spider sensory system.* Nature, 2014. **516**(7530): p. 222-226.

[47]. Y. Zhou, P. Zhan, M. Ren, G. Zheng, K. Dai, L. Mi, C. Liu, and C. Shen, *Significant Stretchability Enhancement of a Crack-Based Strain Sensor Combined with High Sensitivity and Superior Durability for Motion Monitoring.* ACS Appl Mater Interfaces, 2019. **11**(7): p. 7405-7414.

[48]. Heng Zhang, Dan Liu, Jeng-Hun Lee, Haomin Chen, Eunyoung Kim, Xi Shen, Qingbin Zheng, Jinglei Yang, and Jang-Kyo Kim, *Anisotropic, Wrinkled, and Crack-Bridging Structure for Ultrasensitive, Highly Selective Multidirectional Strain Sensors.* Nano-Micro Letters, 2021. **13**(1): p. 122.

[49]. Xi Wang, Qiao Li, and Xiaoming Tao, *Sensing mechanism of a carbon nanocomposite-printed fabric as a strain sensor.* Composites Part A: Applied Science and Manufacturing, 2021. **144**: p. 106350.

[50]. John G. Simmons, *Electric Tunnel Effect between Dissimilar Electrodes Separated by a Thin Insulating Film.* Journal of Applied Physics, 1963. **34**(9): p. 2581-2590.